Supplemental material

Hydrochlorothiazide improves cardiac function and remodeling in rats with heart failure by inhibiting CAII and NHE1

Jinghong Luo[1,2,3], Juncong Li[1], Jizhang Ye[2], Shudan Chen[2], Qingchun Zeng[1*]

[1]State Key Laboratory of Organ Failure Research, Department of Cardiology, Nanfang Hospital, Southern Medical University, Guangzhou, China

[2]Department of Geriatrics, Huizhou Central People's Hospital, Huizhou, China

[3]Centre for scientific research, Huizhou Municipal central Hospital, Huizhou, China

Correspondence: Dr. Qingchun Zeng, State Key Laboratory of Organ Failure Research, Department of Cardiology, Nanfang Hospital, Southern Medical University, Guangzhou 510080, China, E-mail: qingchunzeng@smu.edu.cn

Supplemental methods

Animals and treatment

Male Sprague–Dawley rats weighing 200–250 g were obtained from the Experimental Animal Center of Nanfang Medical University (Guangzhou, China). All animal experiments were performed with the approval of the Experimental Animal Ethical Committee at this university and conducted based on the Guide for the Care and Use of Laboratory Animals (NIH publication No. 85-23, revised 1996). Rats were anesthetized by intraperitoneal (ip) administration of 3% pentobarbital sodium (45 mg/kg) and then intubated and ventilated via a tracheal cannula using a constant-volume rodent ventilator (tidal volume: 3.0 mL; respiratory rate: 70 cycles/min). Following left thoracotomy and pericardiotomy, a large left ventricular anterior transmural myocardial infarction (MI) was induced by permanent left anterior descending coronary artery ligation at 2–3 mm from the origin with a 7–0 silk suture. The chest was closed immediately after verifying the color change in the ischemic area. A similar surgical procedure was performed in sham-operated rats without coronary artery ligation. Two weeks post-surgery, left ventricular dimensions and EF were measured by echocardiography in surviving coronary ligated and sham-operated rats. Forty rats were matched by cardiac functions using echocardiography and

randomly divided into three experimental groups: sham-operated group (n = 10), HF group (n = 15), and hydrochlorothiazide group (12.5 mg/(kg·day), n = 15). Drugs or vehicles were administered orally by gavage for 6 weeks. The drug doses were based on observations from previous studies.

Echocardiogram evaluation

Echocardiography was performed to evaluate the cardiac geometry and systolic and diastolic functions as previously described. The high-resolution Vevo2100 ultrasound system (Visual Sonics, USA) was used for echocardiography, which was equipped with an MS250 transducer. In brief, the rats were anesthetized with 2.0% isoflurane until the heart rate stabilized at 400–500 beats per minute. Parasternal long-axis images were acquired in B-mode with an appropriate position of the scan head to identify the maximum left ventricular (LV) length. In this view, the M-mode cursor was positioned perpendicular to the maximum LV dimension in end-diastole and systole. M-mode images were obtained to measure wall thickness and chamber dimensions. LVEF and LV fractional shortening were calculated automatically. The measurements were averaged over three consecutive cardiac cycles. The hemodynamic measurements were conducted 2 days later.

Hemodynamic measurements

A terminal surgical procedure was performed to evaluate LV pressure and contractile properties as described previously. The rats were anesthetized with 2%–3% isoflurane, and the right carotid artery was exposed. A microtip pressure transducer catheter (1.4F; Millar Instruments, TX, USA) was introduced via the right carotid artery into the left ventricle. The heart rate, LV end-systolic pressure (LVESP), left ventricular end-diastolic pressure (LVEDP), and the maximum rising and dropping rates of left ventricular pressure ($\pm dp/dt$) were measured using a commercially available analog-to-digital converter and analyzed using BIOPAC AcqKnowledge Analysis Software (Goleta, CA, USA).

Rat serum assays

The rats were sacrificed, and blood was collected from the abdominal vena cava. Approximately 5 mL of blood was placed in a test tube containing heparin lithium.

The blood samples were centrifuged at 1000*g* and 4°C for 10 min. The plasma was collected immediately and then stored at −80°C for measuring cytokines and electrolyte levels. Plasma potassium, sodium, chlorine, magnesium, and creatinine levels were measured by Wuhan Servicebio biotechnology laboratory. The levels of cytokines [renin, Ang II, aldosterone, Pro-BNP, C-reactive protein (CRP), endothelin 1, MDA, SOD, T-AOC, mitochondrial respiratory chain complex I, and mitochondrial respiratory chain complex IV] were determined using commercially obtained enzyme-linked immunosorbent assay (ELISA) kits (R&D systems, MN, USA) following the manufacturer's protocols.

Histological assessments

Fresh myocardial tissue samples were washed with normal saline solution, followed by fixation with 4% paraformaldehyde for 24 h. The tissue was then embedded in paraffin and sectioned to 5 μm thickness. After deparaffinization, adjacent sections were stained with Masson trichrome for collagen deposition associated with fibrosis. All images were taken using the CellSens standard system of the inverted microscope. To quantify cardiac fibrosis, 12 fields were randomly selected from 3 cardiac sections and calculated as the percentage of Masson's trichrome positive–stained area to the total myocardial area using ImageJ software as previously described.

Immunohistochemical staining

Immunohistochemical staining of collagen I, collagen III, MCP-1, NCF-1/p47phox, and cytochrome c was performed to determine the myocardial inflammation, fibrosis, oxidative stress, and apoptosis. Briefly, the sections were fixed with 4% paraformaldehyde for 10 min and blocked with hydrogen peroxide and 10% goat serum (Wuhan Servicebio Biotechnology, China) for 10 and 30 min, respectively, at room temperature, and then incubated with the corresponding primary antibodies (Wuhan Servicebio Biotechnology) overnight. After washing with phosphate-buffered saline (PBS) three times, the sections were incubated with anti-rabbit immunoglobulin G–peroxidase conjugate (Proteintech, China) for 30 min at room temperature and developed by adding the substrate Diaminobenzidine (DAB). The images were taken with 400× magnification using the Nikon microscope with CellSens standard software.

For quantitative analysis, 12 fields (3 fields per section and 3 sections) were randomly selected to perform the statistical analysis using the ImageJ software.

Immunofluorescence staining

The paraffin-embedded sections were labeled with primary antibodies overnight for immunofluorescence microscopy, followed by incubation with a suitable fluorophore-conjugated secondary antibody for 1 h. Specifically, rabbit anti-rat-caspase3 antibody (GB11532, 1:500; Servicebio) was used to stain cardiomyocytes. Immunofluorescence images were obtained using an inverted fluorescence microscope (Nikon, Tokyo, Japan) with CellSens standard software. Positive-staining cells in the images were quantified using the ImageJ software. The results were presented as the average number of positive-staining cells in each high power field (HPF). We quantified at least five randomly chosen HPFs per heart section from one rat for all analyses, with at least three rats per indicated group.

TUNEL detection

Autofluorescence was quenched by treating paraffin-embedded sections with PBS/bovine serum albumin (5%) for 2 h before performing terminal deoxynucleotidyl transferase–mediated dUTP nick-end labeling (TUNEL) staining (Servicebio, China) following the manufacturer's protocol to analyze apoptotic myocytes in the heart. The sections were counterstained with Alexa Fluor 594-conjugated WGA (Invitrogen, CA, USA) at 10 μg/mL for 1 h at room temperature to visualize cell membranes. The slides were scanned with the digital slide scanner NanoZoomer 2.0-RS (Hamamatsu, Japan), which allowed an overall view of the samples. The images were digitally captured from the scan slides using the NDP.view2 software (Hamamatsu, Japan).

RNA extraction and quantitative real-time polymerase chain reaction

Total RNA was extracted from tissues and cultured cells following standard protocols using TRIzol reagent (15596026; Invitrogen). Further, 1 μg of total RNA was reverse transcribed into cDNA using a reverse transcription kit (with dsDNase). cDNA (1 μL) was then mixed with quantitative polymerase chain reaction (qPCR) SYBR Master Mix and 0.2 μM primers to finally obtain a mixture of 10 μL, which was subjected to qRT-PCR following the manufacturer's protocols (LightCysler 480; Roche). The

fluorescence curves were analyzed using LightCycler 96 software (Version 1.1; Roche). The primers used to determine the expression of specific genes are listed in Table S2. The relative mRNA expression of specific genes was quantified using the comparative ΔΔCT method and normalized to GAPDH.

Protein isolation and Western blotting

Fresh frozen ventricular tissue (20 mg) or cultured cells were homogenized in RIPA buffer (Phygene, China). A protease and phosphatase inhibitor cocktail (Sigma–Aldrich, USA) was added to the lysis buffer immediately before lysis. The samples were centrifuged at 12,000*g* and at 4°C for 15 min, and the supernatant was collected for further analysis. The protein concentrations were determined using a BCA Protein Assay Kit (Biosharp, Hangzhou, China). For Western blotting, an equal amount of protein (10–30 μg) was separated by 10% sodium dodecyl sulfate–polyacrylamide gel electrophoresis and transferred onto a 0.22-μm polyvinylidene fluoride membranes (Millipore, USA). The membranes were blocked for 1.5 h at room temperature in Tris-buffered saline and 0.1% Tween-20 containing 5% skimmed milk and then incubated with primary antibodies in the same buffer at 4°C overnight, followed by incubation with HRP-conjugated secondary antibodies (1:10,000 in 5% milk) at room temperature for 1.5 h. Specific protein bands were detected using ECL detection reagent (Biosharp, Hangzhou, China). Western blot results were densitometrically quantified using ImageJ software, and the intensity values were normalized to GAPDH. The antibodies used were as follows: Bax (1:500; Servicebio), caspase3 (1:500; Proteintech), cytochrome c (1:500; Servicebio), NCF-1/p47phox (1:500; Servicebio), NADPH oxidase 2 (NOX2)/p67phox (1:800; Proteintech), SOD (1:10,000; Proteintech), collagen I (1:500; Servicebio), collagen II (1:500; Servicebio), NHE1 (1:3000; Proteintech), NCX1 (1:250; Solarbio), NF-κB p65 (1:1500; Proteintech), p38 mitogen–activated protein kinase (p38 MAPK) (1:1000; Proteintech), and c-Jun N-terminal kinase (JNK) (1:2000; Proteintech).

Cell culture and drug treatments

The embryonic rat-heart-derived H9C2 cells (Pricella, Wuhan, China) were propagated in high-glucose Dulbecco's modified Eagle's medium supplemented with

10% FBS, 100 U/mL penicillin, and 100 mg/mL streptomycin at 37°C in a humidified atmosphere of 5% CO_2 and 95% air. Passages 3 to 5 of H9C2 cells at 70%–80% confluence were used for experiments. The cells were serum-starved for 1 h before stimulation. First, we verified the effects of different concentrations of hydrochlorothiazide on cell inflammation, oxidative stress, and apoptosis. The sources and doses of the drug were as follows: control group (0.005% dimethylsulfoxide), angiotensin (Ang) II group (1 μmol/L, A32360; Acmec, China), Ang II + hydrochlorothiazide low-dose group (5 μmol/L, F-B22093; Alfa Aesar, USA), Ang II + hydrochlorothiazide medium-dose group (10 μmol/L), and Ang II + hydrochlorothiazide high-dose group (20 μmol/L). After 24 h of drug intervention, the total RNA and protein of cells were extracted for qPCR and Western blot detection. Second, the effects of hydrochlorothiazide, NHE1 inhibitor (cariporide) and antioxidant [*N*-acetyl-L-Cysteine (NAC)] on cell inflammation, oxidative stress, and apoptosis were compared. The sources and doses of the drugs were as follows: control group, Ang II group, Ang II + hydrochlorothiazide (10 μmol/L), Ang II + cariporide group (10 μmol/L, C84880; Acmec), and Ang II + NAC group (10 μmol/L, N27390; Acmec). After 24 h of drug intervention, the total protein of cells was extracted for Western blot detection.

Reactive oxygen species detection

H9C2 cells at 50%–70% confluence were used for experiments. The experimental procedures were performed using the reactive oxygen species (ROS) detection kit (BL714A, Biosharp) following the manufacturer's protocols. Briefly, the cell culture medium was aspirated, and the 2'-7'dichlorofluorescin diacetate (DCFH-DA) working solution was added after washing with PBS twice and placed in the incubator for 30 min. After incubation, the DCFH-DA working solution was blotted off, and after washing with PBS twice, the cells were placed under a fluorescence microscope (Nikon, Tokyo, Japan) with CellSens standard software for observation and imaging.

Mitochondrial membrane potential detection

H9C2 cells at 50%–70% confluence were used for experiments. The experimental procedures were performed using the mitochondrial membrane potential assay kit

(JC-1, BL711A; Biosharp) following the manufacturer's protocols. Briefly, the medium was aspirated, and JC-1 staining working solution was added after washing with PBS and incubated for 20 min in a cell culture incubator. At the end of incubation, the cells were washed two times with JC-1 staining buffer and placed under a fluorescence microscope for observation and imaging. The declining degree of cell membrane potential in each group was evaluated by calculating the green and red fluorescence proportions using the ImageJ software.

Transfection of small interfering RNA and gene overexpression plasmid

The siRNA of the target gene was constructed to understand the effects of carbonic anhydrase (CA) II and NHE1 on inflammation, oxidative stress, and apoptosis. Rat small interfering RNAs (siRNAs) against CAII and NHE1 (R10043.8) were purchased from Ribobio Biotechnology(China). The interference sequences are listed in Table S3. H9C2 cells were plated into 6-well plates at 50%–60% confluence and infected with SiRNA using Lipofectamine 3000 (Invitrogen) following the manufacturer's protocol. Further, 24 h after transfection, the proteins were extracted for Western blot analysis after an additional 24 h of Ang II treatment. NHE1 overexpression plasmids were constructed to transfect H9C2 cells by lentivirus (GZF20220806; Tsingke Biotechnology, China) to further understand the inhibition of NHE1 by hydrochlorothiazide. Further, 48 h after transfection, an intervention with hydrochlorothiazide was performed for 24 h. The downstream effector proteins of inflammation, oxidative stress, and apoptosis were detected by Western blot analysis.

Statistical analyses

The quantitative results were expressed as the means ± SD. The normality and the homogeneity of variance of the data were examined. For data that showed a normal distribution and homogeneity of variance, the differences between the two groups were compared with a two-tailed Student *t* test. The differences among three or more groups were analyzed using one-way analysis of variance (ANOVA) followed by Bonferroni analysis (for data meeting homogeneity of variance) or Tamhane's T2 analysis (for data demonstrating heteroscedasticity). A Kruskal–Wallis test plus a *post hoc* analysis (Dunn's multiple comparison test) was used for variables not passing a

normality or equal variance test. The two-way ANOVA (ordinary or mixed effects) with Sidak's or Tukey's *post hoc* test was used when appropriate. Graphs were created using Prism 5.0 (GraphPad Software), and statistical analysis was performed using SPSS Statistics 22.0. A P value <0.05 indicated a statistically significant difference.

Supplemental TableI

List of reagents and chemicals.

Reagents or resources	Source	Identifier
Antibodies		
Bax	Servicebio	GB12690
CA II	Servicebio	GB111972
NCF1/p47phox	Servicebio	GB11724
NHE1	Proteintech	67363-1-lg
NCX1	Solarbio	K106450P
SOD2	Proteintech	66474-1-lg
NOX2/p67phox	Proteintech	15551-1-AP
Caspase3	Proteintech	66470-2-lg
GAPDH	Proteintech	60004-1-lg
P38MAPK	Proteintech	66234-1-lg
JNK	Proteintech	66210-1-lg
Collagen I	Servicebio	GB11022
NF-κB P65	Proteintech	66535-1-lg
Cytochrome C	Servicebio	GB11080
HRP-conjugated Goat Anti-Mouse IgG	Proteintech	SA00001-1
HRP-conjugated Goat Anti-Rabbit IgG	Proteintech	SA00001-2
Chemicals		
10%SDS	Biosharp	BL517A

Tris-HCL (PH6.8)	Phygene	PH0365
Tris-HCL (PH8.8)	Biosharp	BL515A
10%APS	Phygene	PH1808
Glycine	Phygene	PH0604
Tris-base	Phygene	PH0713
30% acrylamide/ methylene solution (29:1)	Biosharp	BL513B
TEMED	Regent Biol	PE0157
TBS	Servicebio	G0001
Skim milk powder	Phygene	PH1519
BSA-V	Solarbio	A8020
Triton X-100	Solarbio	T8200
Tween-20	Solarbio	9005-64-5
4% Paraformaldehyde	Labcoms	LA1110
N-Acetyl-L-Cysteine	Acmec	N27390
Cariporide	Acmec	C84880
Hydrochlorothiazide	Alfa Aesar	F-B22093
Angiotensin II	Acmec	A32360
Critical commercial Assays		
BCA protein concentration assay kit	Biosharp	BL521A
RIPA buffer	Phygene	PH0316
SDS-PAGE Sample Loading Buffer	Solarbio	P1016
Western Protein Marker	Biosharp	BL713A
phosphatase inhibitors	Biosharp	BL615A
Mitochondrial Membrane Potential Detection Kit (JC-1)	Biosharp	BL711A

Reverse Transcription Kit (with dsDNase)	Biosharp	BL699A
TRIzol Reagent	Invitrogen	15596026
SYBR Green qPCR Mix	Biosharp	BL698A
ECL chemiluminescent substrate	Biosharp	BL523A
ROS detection kit	Biosharp	BL714A
TUNEL apoptosis detection kit (FITC)	Phygene	PH1456

Supplemental TableII

Primers used for the RT-qPCR assays in this study

Primers for mouse RT-qPCR		
Gene	Forward primers (5'- 3')	Reverse primers (5'- 3')
GAPDH	CTGGAGAAACCTGCCAAGTATG	GGTGGAAGAATGGGAGTTGCT
NCX1	CCGCACTGTGCATCGACTAC	TGTTGGGAGGCGCAGAGTA
Bax	TTTGCTACAGGGTTTCATCCAG	GTTGTTGTCCAGTTCATCGCC
Bcl2	TTGTGGCCTTCTTTGAGTTCG	GCATCCCAGCCTCCGTTAT
Caspase3	CTGGACTGCGGTATTGAGACA	CGGGTGCGGTAGAGTAAGC
SOD2	TCTGGACAAACCTGAGCCCTAA	GAACCTTGGACTCCCACAGACA
CAII	GTGGAGCAAACTGGGTAGTGAAT	AAGATACCGTTGCTCCCTGTG
NHE1	CAGCCTTCACCTCACGATTTAC	ACTTGATGGTGGTGTGGGATTT
P67phox	TAGGCTGTTCCGTCCAAATGA	AACCGTAGCCTTGCCCAGATA
CollagenI	CGTGGAAACCTGATGTATGCTTG	CCTATGACTTCTGCGTCTGGTGA
P38MAPK	CGGTGTGTGCTGCTTTTGAT	CTGTAGGTCCTTTTGGCGTG
JNK	TGAGCAGAAGTAAACGTGACAACAA	ATCATAAGCTGCACACACTATTCCT
NF-κB p65	CAGATACCACTAAGACGCACCC	CTCCAGGTCTCGCTTCTTCACA
NCF1	ATCGCTGACTACGAGAAGGGT	GCTTTGATGGTTACATACGGTTC

All primer sets worked under identical quantitative PCR cycling conditions with similar efficiencies to obtain simultaneous amplification in the same run. Sequences were taken from GenBank and all accession numbers are denoted.

Supplemental Table III

Sequence of siRNA

Gene	Sequence
CAII	CCAAGAGCATTGTCAACAA
	TGAAGAACAGAAAGATCAA
	TGAAGAACAGAAAGATCAA
NHE1	GCGAGCAGATCAATAACAT
	GCAAAGTCCTTGGGCTAAA
	CCGTCTCAACTGTCTCTAT

Supplemental FigureI

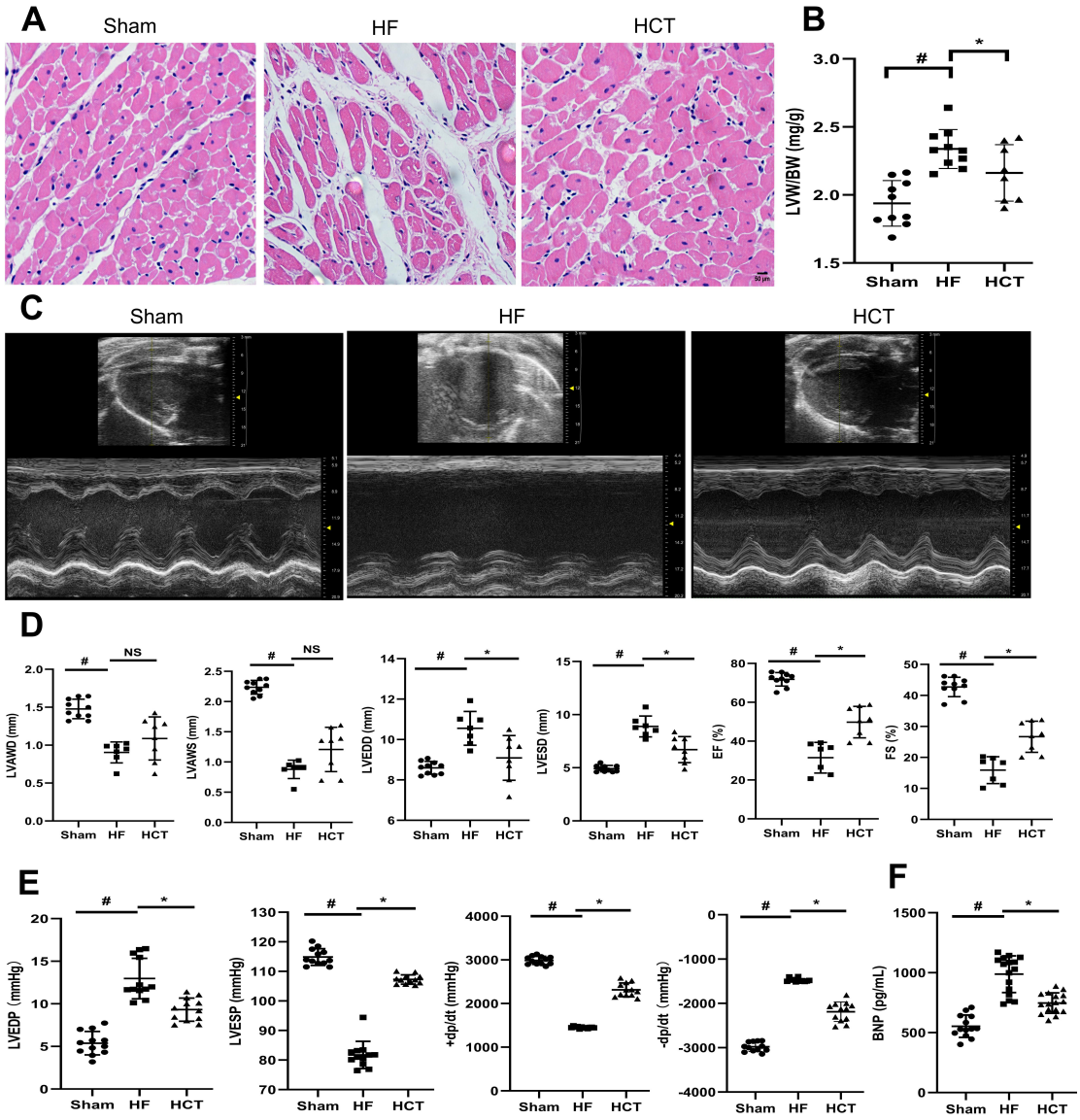

Hydrochlorothiazide can improve cardiac function in rats with heart failure.

A. Representative images of hematoxylin and eosin (H&E) staining of heart sections after 6 weeks of drug intervention for tissue morphology analysis.

B. HF group rats showed an increase of LVW/BW, indicating more severe pathological remodeling, but hydrochlorothiazide can significantly reduce it. $p<0.05$. n=8-10.

C. Representative echocardiograms images obtained from 6 weeks after drug intervention.

D. Echocardiographic assessment of cardiac function in rats. $p<0.05$. n=7-10.

E. Hemodynamic detection was used to evaluate the cardiac function. $p<0.05$. n=12-15.

F. The levels of plasma BNP were detected by enzyme-linked immunosorbent assay (n=13-16).

Data are presented as mean±SEM. #P<0.05, compared with Sham group, *P<0.05. NS: not significant, compared with HF group. Data were analyzed using one-way ANOVA followed by Bonferroni multiple comparison test.

HF: heart failure; HCT: hydrochlorothiazide; LVW/BW: Left ventricular weight to body weight ratio; LVAWD: Left ventricular anterior wall thickness in diastole; LVAWS: Left ventricular anterior wall thickness in systolic; LVEDD: left ventricular end diastolic dimension; LVESD: left ventricular end systolic dimension; EF: Ejection fraction; FS: fractional shortening; LVEDP: left ventricular end diastolic pressure； LVESP: left ventricular end systolic pressure; ±dp/dt: the maximum left ventricular pressure increase and decrease rate.

Supplemental Figure II

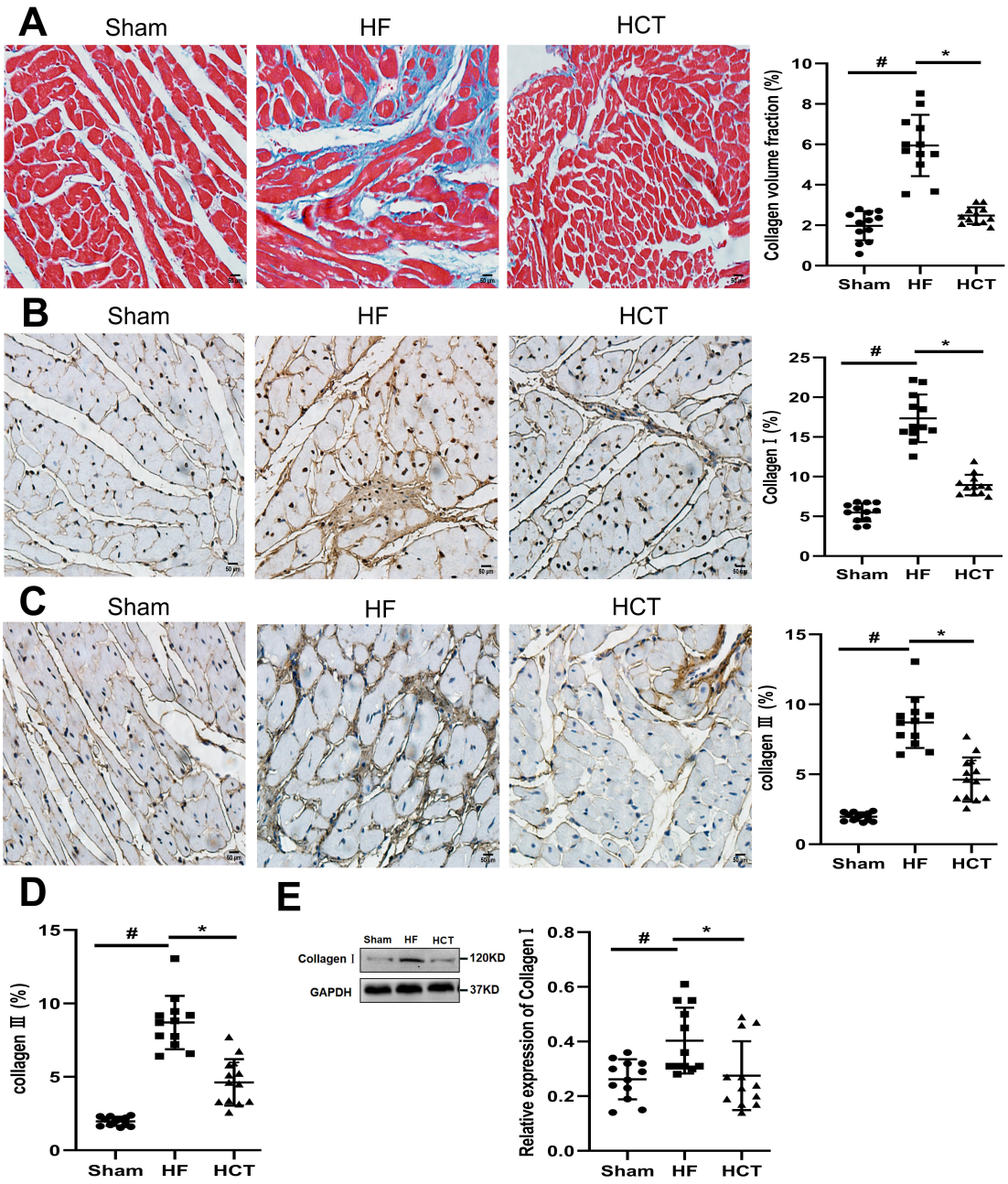

Hydrochlorothiazide can improve myocardial fibrosis in rats with heart failure.

A. Representative macroscopic view of masson's trichrome staining of non- infarcted myocardium interstitium. Images were taken at 400 magnification. Scale bars, 50μm. The quantitative analysis of Masson's trichrome stained as the total collagen volume fraction (CVF).

B and C. Representative immunohistochemistry analyses of collagen I and collagen III in both groups (bar=50 μm).

D. Cardiac fibrotic gene expression was significantly downregulated in hydrochlorothiazide group, as determined by qPCR (n=3). mRNA expression levels were normalized to those of GAPDH.

E. Representative western blot and quantification of collagen I protein. GAPDH were used as a loading control.

Data are presented as mean±SEM. #P<0.05, compared with Sham group, *P<0.05, compared with HF group. Data were analyzed using one-way ANOVA followed by Bonferroni multiple comparison test.

Supplemental Figure III

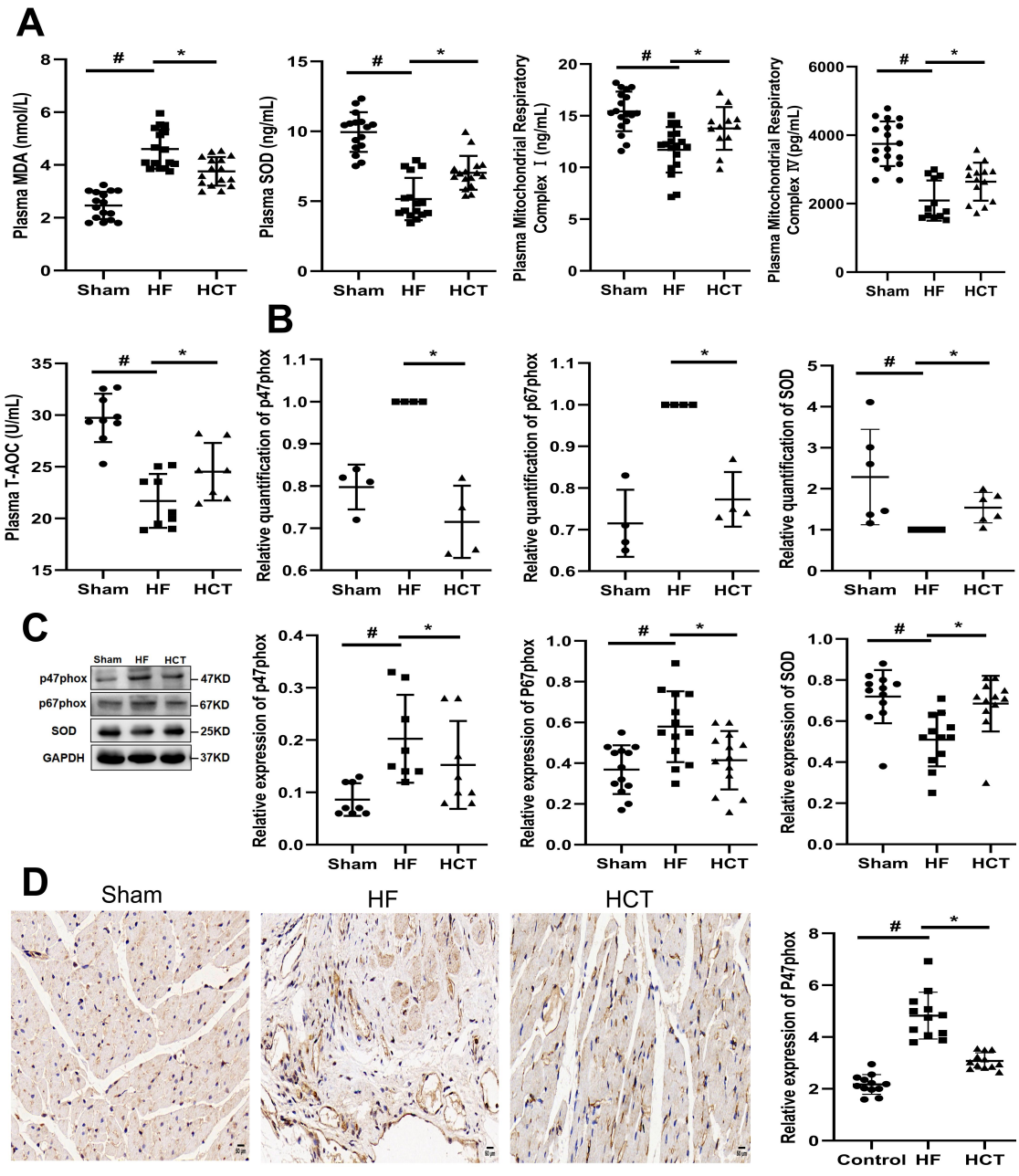

Hydrochlorothiazide can reduce oxidative stress.

A. The levels of plasma oxidative stress indicators were detected by enzyme-linked immunosorbent assay (n=7-18).

B and C. Oxidative stress indicators (p47phox, p67phox and SOD) expression were analyzed by q PCR and western blotting in the non- infarcted myocardium(n=4-13). mRNA and protein expression levels were normalized to those of GAPDH.

D. Representative immunohistochemistry analyses of p47phox in both groups (bar=50 μm).

Data are presented as mean±SEM. #P<0.05, compared with Sham group, *P<0.05, compared with HF group. Data were analyzed using one-way ANOVA followed by Bonferroni multiple comparison test.

MDA: malondialdehyde; SOD: Superoxide dismutase; T-AOC: Total antioxidant capacity.

Supplemental Figure IV

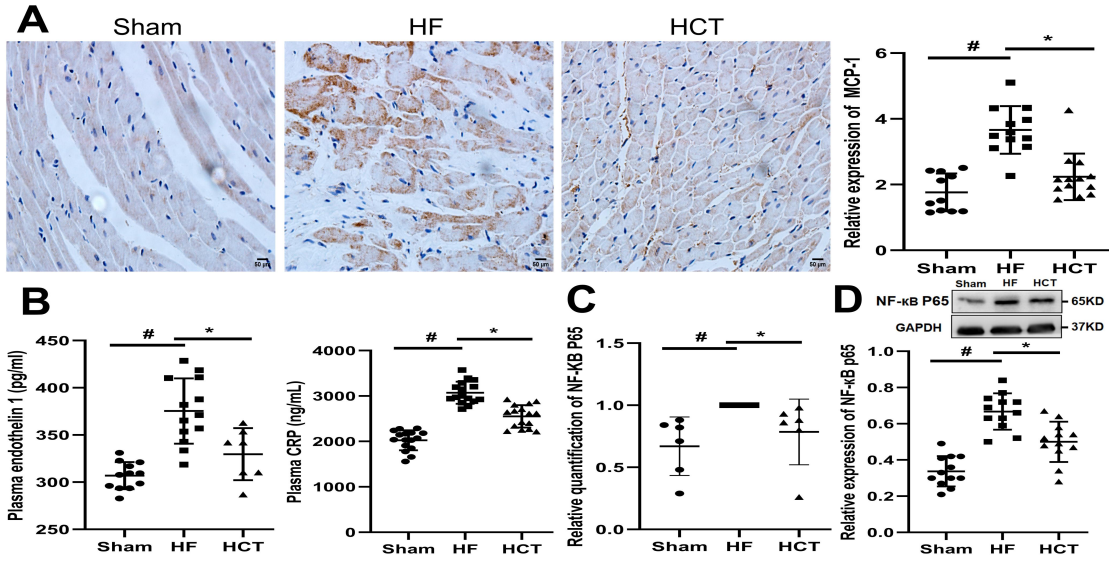

Hydrochlorothiazide can reduce inflammation in rats with heart failure.

A. Representative immunohistochemistry analyses of MCP-1 in both groups (bar=50 μm).

B. The levels of ET-1 and CRP were detected by enzyme-linked immunosorbent assay (n=7-16).

C and D. NF-κB p65 expression was analyzed by qPCR and western blotting in the non-infarcted myocardium (n=4-12). mRNA and protein expression levels were normalized to those of GAPDH.

Data are presented as mean±SEM. $^{\#}P<0.05$, compared with Sham group, $*P<0.05$, compared with HF group. Data were analyzed using one-way ANOVA followed by Bonferroni multiple comparison test.

MCP-1: Monocyte chemoattractant protein-1; CRP: C-reactive protein.

Supplemental Figure V

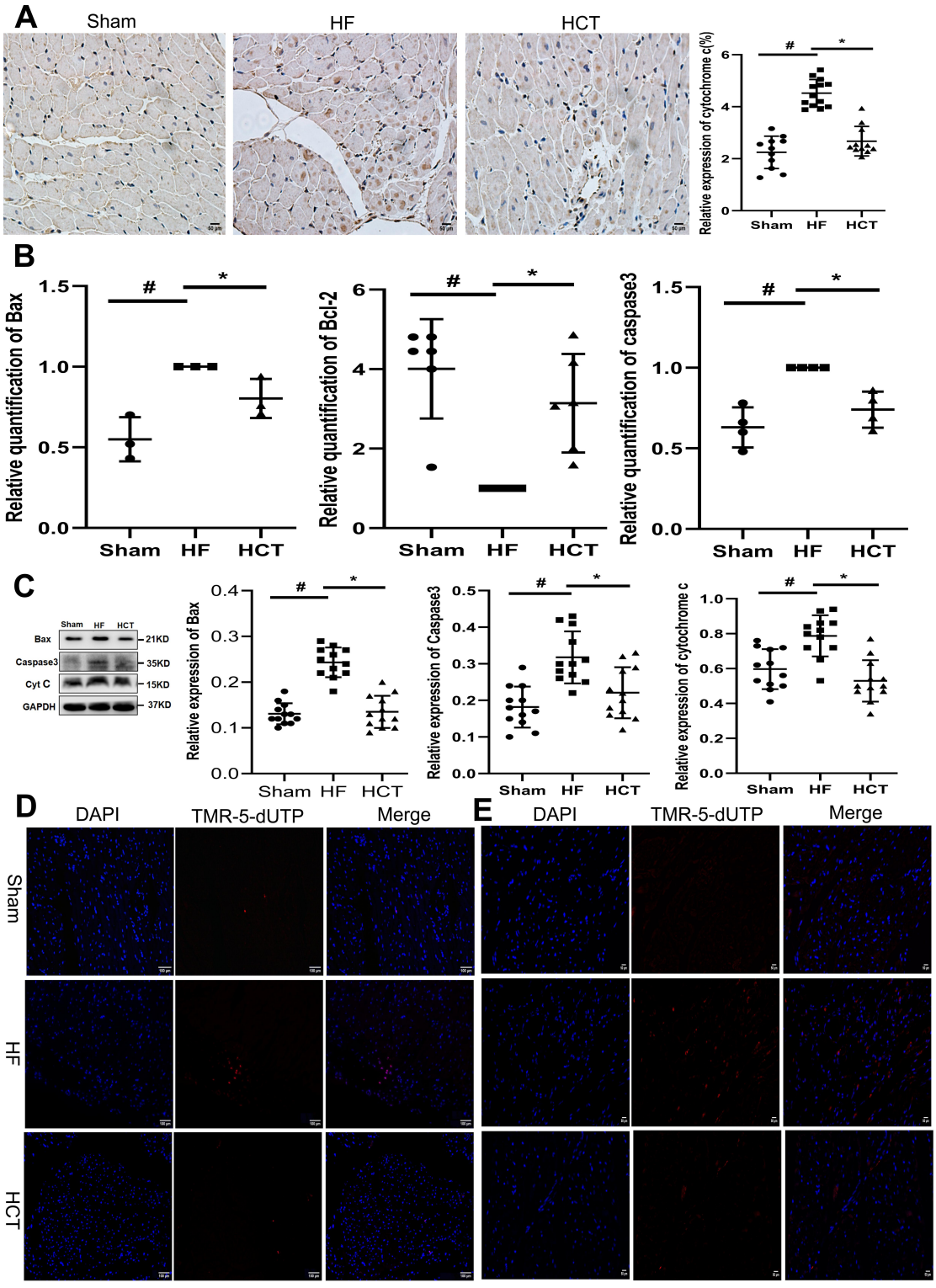

Hydrochlorothiazide attenuates cardiomyocyte apoptosis.

A. Representative immunohistochemistry analyses of cytochrome C in both groups (n=12).

B. Bax、Bcl-2、caspase3 mRNA expression were analyzed by q PCR (n=3-6). mRNA expression levels were normalized to those of GAPDH.

C. Bax、caspase3、cytochrome C protein expression were analyzed by western blot (n=12). Protein expression levels were normalized to those of GAPDH.

D. TUNEL assay was used to detect the apoptosis of cardiomyocytes in heart failure rats.

E. Representative immunofluorescent staining of apoptosis marker (caspase3) in sections of heart from rat. Scale bar, 50 μm.

Data are presented as mean±SEM. #P<0.05, compared with Sham group, *P<0.05, compared with HF group. Data were analyzed using one-way ANOVA followed by Bonferroni multiple comparison test.

Supplemental Figure VI

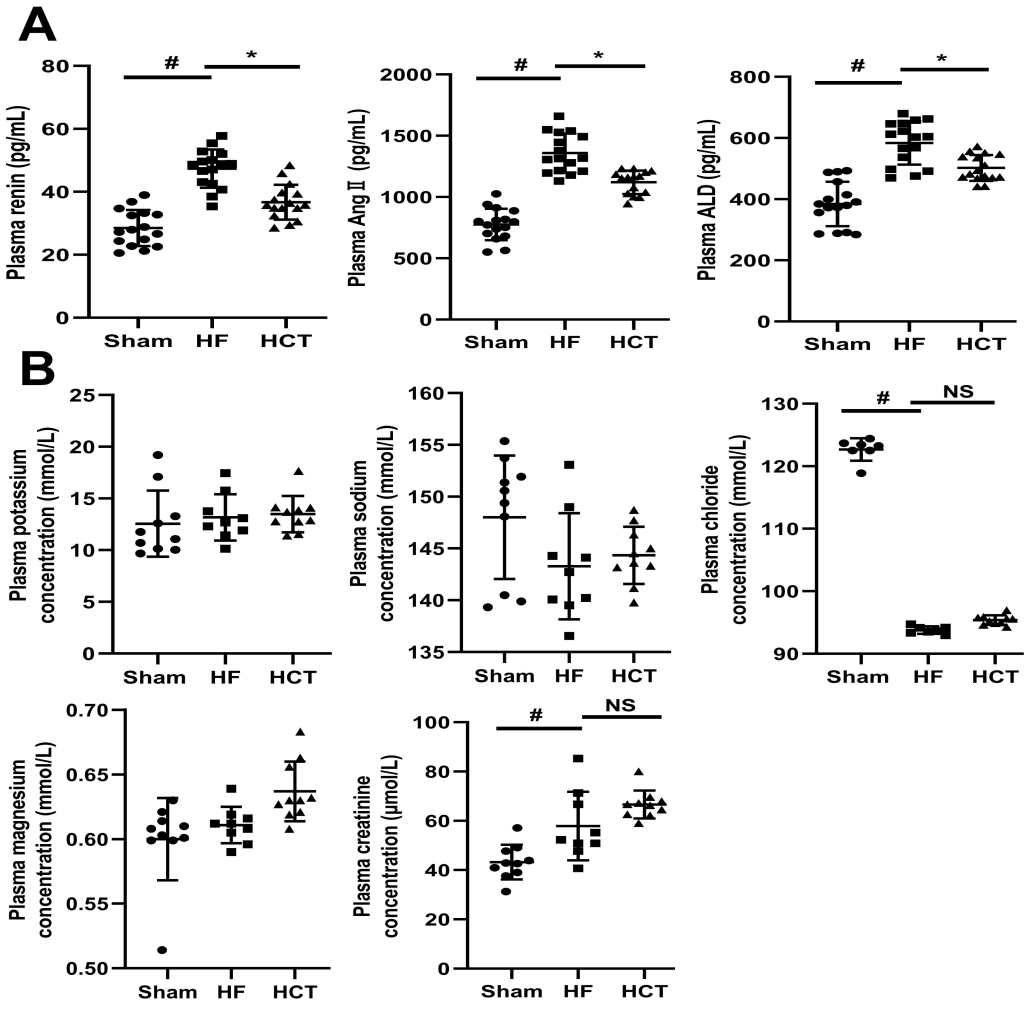

Effects of hydrochlorothiazide on RASS, electrolytes, and renal function.

A. The plasma levels of Renin、Ang II、ALD were detected by enzyme-linked immunosorbent assay (n=16).

B. The plasma electrolyte (Potassium, sodium, chloride, magnesium) and creatinine levels were determined by biochemical method (n=16).

Data are presented as mean±SEM. $^{\#}P<0.05$, compared with Sham group, $*P<0.05$. NS: not significant, compared with HF group. Data were analyzed using one-way ANOVA followed by Bonferroni multiple comparison test.

AngII: Angiotensin II; ALD: aldosterone.

Supplemental Figure VII

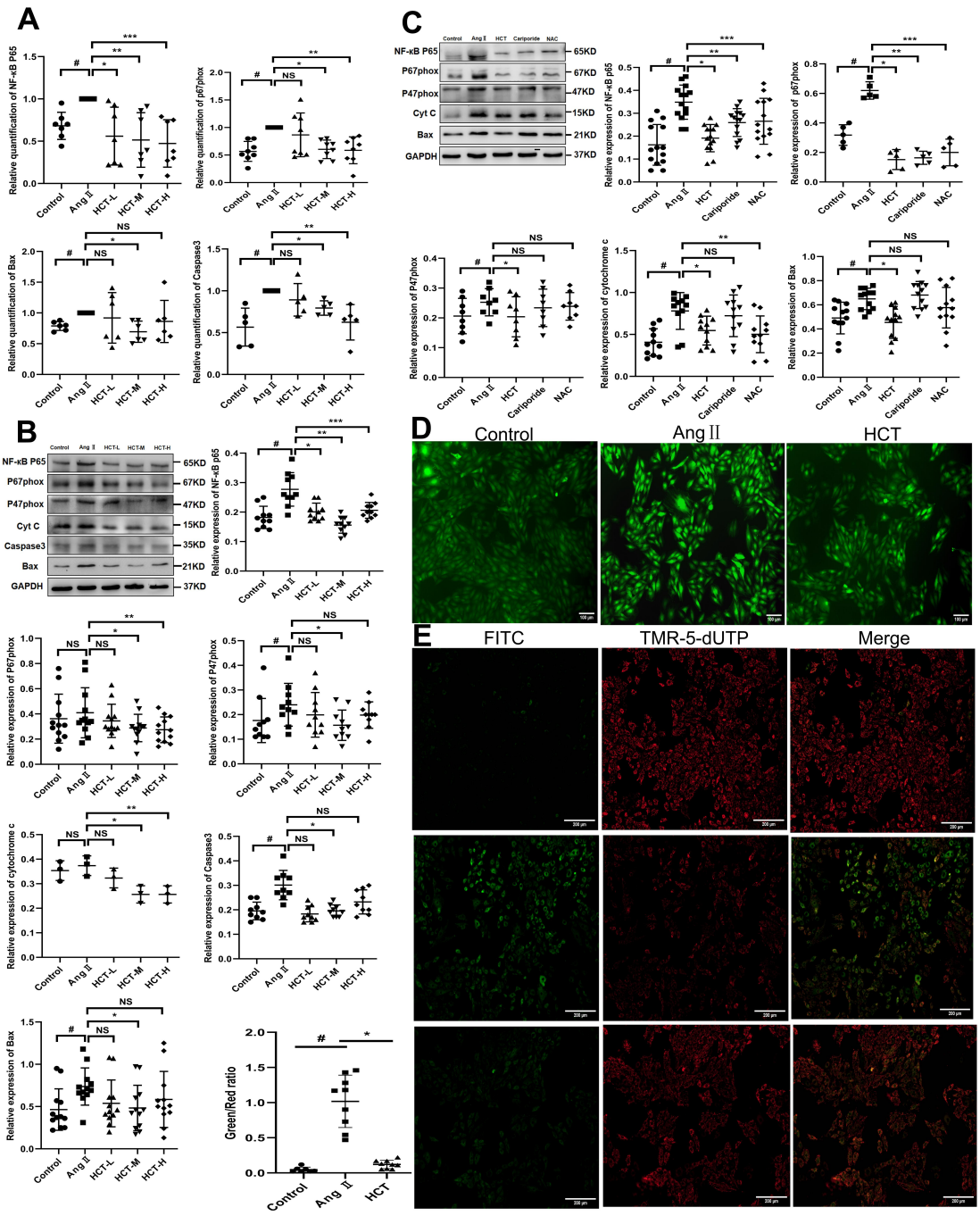

Effects of hydrochlorothiazide on inflammation, oxidative stress and apoptosis of H9C2 cardiomyocytes.

A and B.The effects of different concentrations of hydrochlorothiazide on the mRNA and protein expression of indicators of inflammation, oxidative stiffness, and apoptosis (NF-κB p65, p47phox, p67phox, Bax, cytochrome C) in H9C2 cells were determined by qPCR and Western blot analysis. mRNA and protein expression levels were normalized to those of GAPDH.

C. Protein expression of inflammation, oxidative stress, apoptosis in cardiomyocytes treated with hydrochlorothiazide, NHE1 inhibitor (cariporide), antioxidant (NAC) were compared.

D.Typical picture of the effect of hydrochlorothiazide on ROS production in cardiomyocytes.

E.The JC-1 probe was applied to detect the effect of hydrochlorothiazide on mitochondrial membrane potential in cardiomyocytes.

Data are presented as mean±SEM. $^{\#}P<0.05$, compared with Control group, $^{*}P<0.05$, $^{**}P<0.05$, $^{***}P<0.05$, NS: not significant, compared with AngII group. Data were analyzed using one-way ANOVA followed by Bonferroni multiple comparison test. Cyt C: cytochrome C; NAC: N-acetylcysteine; HCT-L: Hydrochlorothiazide low dose; HCT-M: Hydrochlorothiazide medium dose; HCT-H: Hydrochlorothiazide high dose.

Supplemental Figure VIII

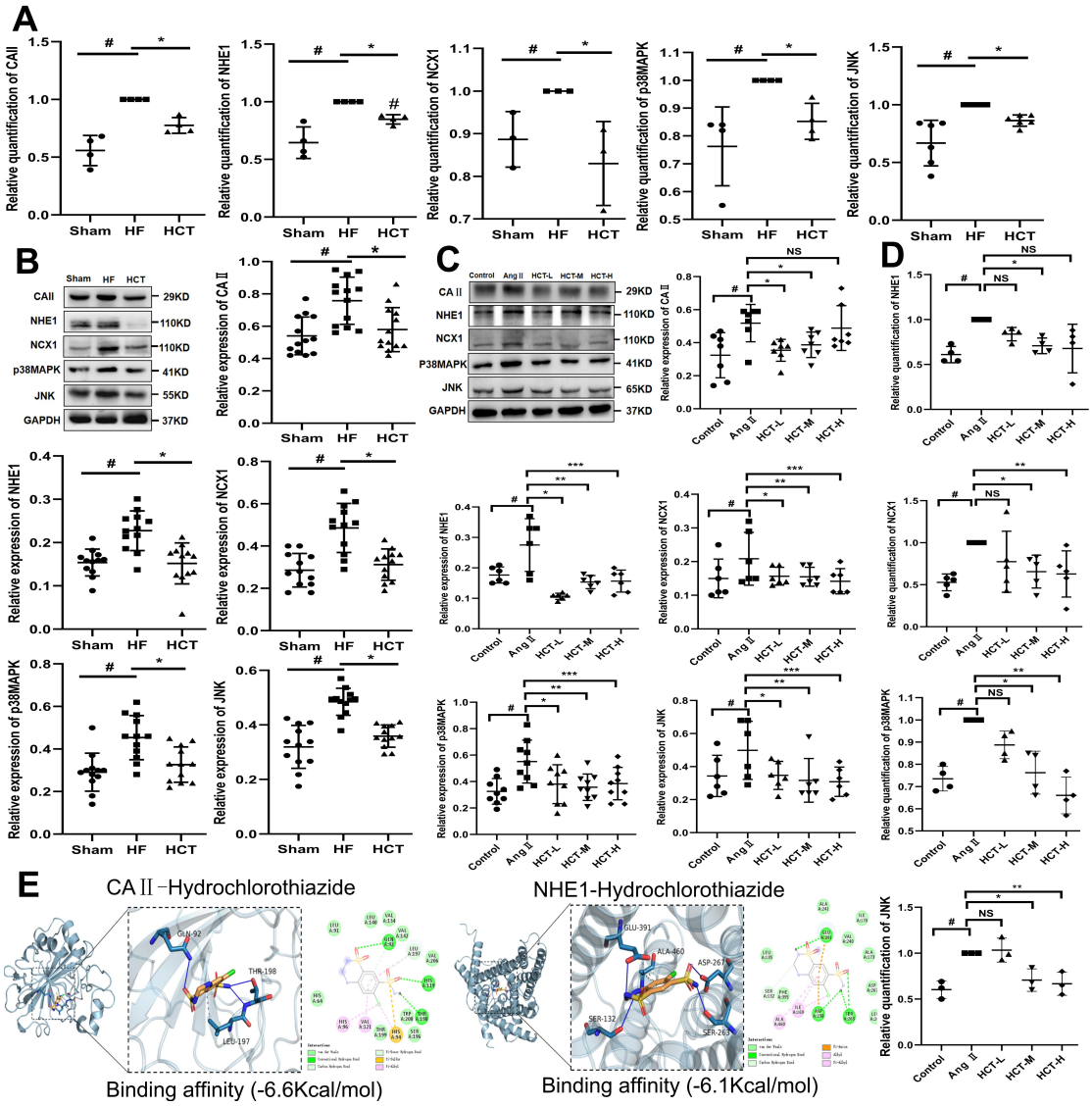

Inhibition of CAII, NHE1 and effects on p38 MAPK / JNK signaling by hydrochlorothiazide.

A. The levels of mRNA expression of CAII, NHE1 and p38 MAPK / JNK signaling pathways in heart failure rats treated with hydrochlorothiazide were determined by qPCR.

B. The levels of protein expression of CA II, NHE1 and p38 MAPK/JNK signaling pathways in heart failure rats treated with hydrochlorothiazide were determined by western blot.

C. The levels of protein expression of CA II, NHE1 and p38 MAPK/JNK signaling pathways in H9C2 cells treated with various concentrations of hydrochlorothiazide were determined by Western blot analysis.

D. The levels of mRNA expression of NHE1, NCX1 and p38 MAPK/JNK signaling pathways in H9C2 cells treated with various concentrations of hydrochlorothiazide were determined by qPCR.

E. Molecular docking simulation approach to explore the binding effect of hydrochlorothiazide on CA II and NHE1 in cardiomyocytes.

F. Data are presented as mean±SEM. $^{\#}P<0.05$, compared with Sham group. $*P<0.05$, compared with HF group (A and B). $^{\#}P<0.05$, compared with Control group, $*P<0.05$, $**P<0.05$, $***P<0.05$, NS: not significant, compared with AngII group (C and D). Data were analyzed using one-way ANOVA followed by Bonferroni multiple comparison test.

Supplemental Figure IX

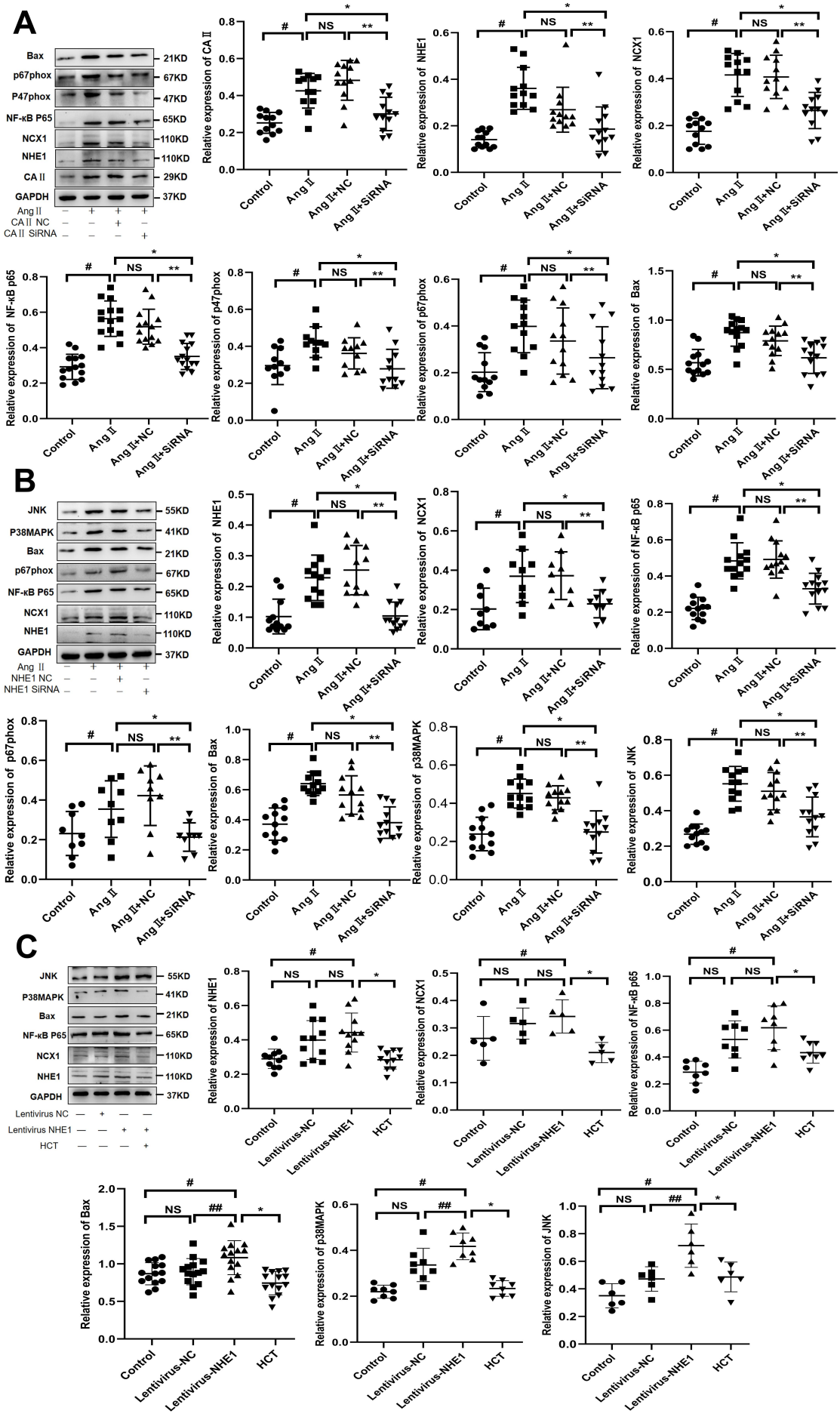
A
Bax
p67phox
P47phox
NF-κB P65
NCX1
NHE1
CA Ⅱ
GAPDH
21KD
67KD
47KD
65KD
110KD
110KD
29KD
37KD
Ang Ⅱ
CA Ⅱ NC
CA Ⅱ SiRNA
Relative expression of CA Ⅱ
Relative expression of NHE1
Relative expression of NCX1
Relative expression of NF-κB p65
Relative expression of p47phox
Relative expression of p67phox
Relative expression of Bax
Control
Ang Ⅱ
Ang Ⅱ+NC
Ang Ⅱ+SiRNA
B
JNK
P38MAPK
Bax
p67phox
NF-κB P65
NCX1
NHE1
GAPDH
55KD
41KD
21KD
67KD
65KD
110KD
110KD
37KD
Ang Ⅱ
NHE1 NC
NHE1 SiRNA
Relative expression of NHE1
Relative expression of NCX1
Relative expression of NF-κB p65
Relative expression of p67phox
Relative expression of Bax
Relative expression of p38MAPK
Relative expression of JNK
C
JNK
P38MAPK
Bax
NF-κB P65
NCX1
NHE1
GAPDH
55KD
41KD
21KD
65KD
110KD
110KD
37KD
Lentivirus NC
Lentivirus NHE1
HCT
Relative expression of NHE1
Relative expression of NCX1
Relative expression of NF-κB p65
Relative expression of Bax
Relative expression of p38MAPK
Relative expression of JNK
Control
Lentivirus-NC
Lentivirus-NHE1
HCT
#
##
NS
*
**

A and B. H9C2 cells were transfected with siRNA targeting CA II and NHE1 or its scramble control for 24 h. After 24 hours of angiotensin II intervention, protein lysates were used for immunoblots to assess CA II and NHE1 protein level. After successful transfection with SiRNA, the protein expression levels of NCX1, NF-κB p65, p47phox, p67phox and bax were further detected.

C.Through lentivirus infection, NHE1 overexpression H9C2 cells were constructed and cultured for 72 hours. HCT was added to HCT group 48 hours after infection. The protein expression levels of NCX1, NF-κB p65, bax, p38MAPK and JNK were further detected.

Data are presented as mean±SEM. $^{\#}P<0.05$, compared with Control group. $^{*}P<0.05$, $^{**}P<0.05$, compared with AngIIgroup. NS: not significant, compared with AngII group (A and B). $^{\#}P<0.05$, compared with Control group. $^{\#\#}P<0.05$, compared with Lentivirus+NC group. $^{*}P<0.05$, compared with Lentivirus+NHE1 group. NS: not significant, compared with Control group (C). Data were analyzed using one-way ANOVA followed by Bonferroni multiple comparison test.

Supplemental Figure X

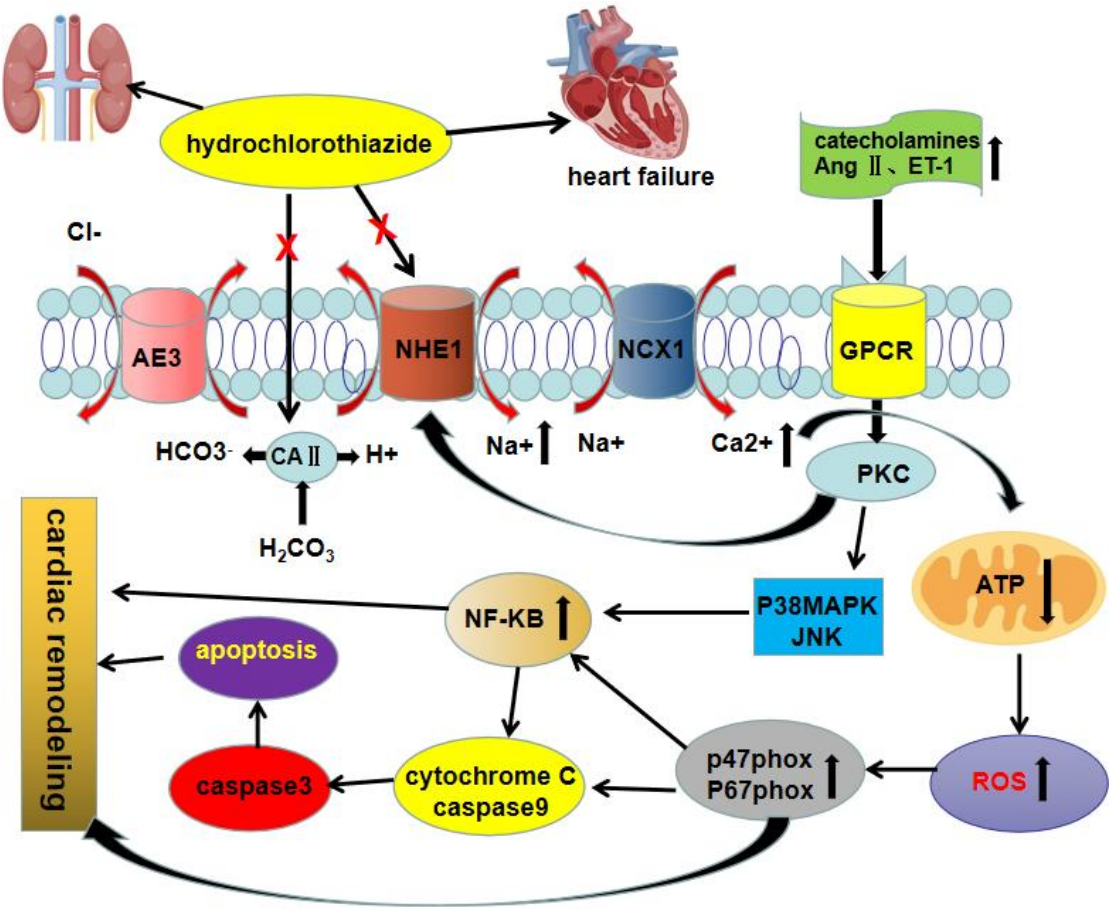

Graphical Abstract. The schematic diagram shows the mechanism of hydrochlorothiazide in improving cardiac remodeling in heart failure. NHE1 is activated during heart failure, which in turn activates downstream NCX1, resulting in intracellular calcium overload, which in turn leads to the aggravation of oxidative stress, inflammatory reaction and apoptosis in myocardial cells, and finally leads to cardiac remodeling and cardiac function damage. Carbonic anhydrase II can catalyze the hydrolysis of intracellular carbonic acid, and the H+produced by hydrolysis plays an important role in the activation of NHE1. Hydrochlorothiazide has the effect of directly binding carbonic anhydrase II and NHE1. By inhibiting carbonic anhydrase II and NHE1, it can reduce the oxidative stress, inflammatory reaction and apoptosis of cardiac myocytes, and ultimately improve cardiac function and cardiac remodeling in rats with heart failure.